

## Dynamic-mechanical behavior of polyethylenes and ethene/ $\alpha$ -olefin-copolymers: Part II. $\alpha$ - and $\beta$ -relaxation

Florian J. Stadler<sup>\*,\*\*,\*†</sup>

<sup>\*</sup>School of Semiconductor and Chemical Engineering, Chonbuk National University,  
664-14, 1-ga Deokjin-dong, Deokjin-gu, Jeonju, Jeonbuk 561-756, Korea

<sup>\*\*</sup>Polymer Materials, Friedrich-Alexander University Erlangen-Nürnberg, Martensstr. 7, D-91058 Erlangen, Germany

(Received 11 May 2010 • accepted 26 August 2010)

**Abstract**—Several ethylene homopolymers and ethene/ $\alpha$ -olefin-copolymers with crystallinities ranging between 85 and 12% were characterized by dynamic-mechanical measurements. The occurring relaxations were correlated to the crystallinity of the polymeric materials and to morphology. The  $\alpha$ -relaxation, being attributed to interlamellar shear, was found to be around 60 °C with activation energies of about 120 kJ/mol in samples with more than 42 % crystallinity. The  $\beta$ -transition shows a much greater variety among the different samples characterized. Its relaxation temperatures vary between –40 and 10 °C with activation energies between 200 and 400 kJ/mol. The  $\alpha$ - and  $\beta$ -relaxation of several quenched samples with crystallinities between 63 and 42 % were found to overlap, thus producing bimodal maxima and different activation energies from the Arrhenius plots. A separation of these overlapping relaxations was only possible by measuring the relaxations over a frequency range of more than three orders of magnitude.

Key words: Polyethylene, Ethene-/ $\alpha$ -olefin-copolymer, Dynamic-mechanical Properties, Activation Energy,  $\alpha$ -Relaxation,  $\beta$ -Relaxation

### INTRODUCTION

Bensason et al. [1] described four different crystalline morphologies observed in homopolyethylene and ethene-/ $\alpha$ -olefin copolymers. The highly lamellar crystallite type IV is found in HDPE with crystallinities above 55%. The medium crystalline type III with crystallinities between 42% and 55% is typically found in LLDPE. For plastomers type samples (30% < x < 42%) a mixture of bundle and lamellar crystallites is found, while almost amorphous elastomer samples (x < 30%, type I) contain only bundle crystallites.

The  $\alpha$ -transition is observed in all semi-crystalline polymers [2]. In polyethylenes, this relaxation is split into two overlapping ones, called the  $\alpha$ - and the  $\alpha'$ -transition, which are both designated to the crystalline phase [3]. The  $\alpha$ -relaxation is reported to take place around 50 °C [3-6], while the  $\alpha'$ -relaxation occurs at temperatures closer to the melting point  $T_m$ . Details on the  $\alpha'$ -relaxation are published in the first part of this article series [7]. The  $\alpha$ -transition is well understood in comparison to the other possible transitions [4,5]. It is attributed to main chain movements along the c-axis of the crystals, which is perpendicular to the roughly planar lamella [8-10]. It is commonly accepted that the mechanism of the  $\alpha$ -relaxation involves shear and reorientation movements along the c-axis of the crystal lamella.

As the relaxation occurs in the crystalline phase, the  $\alpha$ -transition temperature is dependent on the crystallinity and the crystal lamella

thickness. Popli et al. [6] found that for polyethylenes with a crystallinity of 40% the  $\alpha$ -transition temperature measured at 1 Hz increased from 25 to 105 °C, when the lamella thickness decreased from 17.5 nm to 7 nm.

An indirect measure of the lamella thickness is the “linear crystallinity.” It is defined as the third root of the crystallinity ( $x^{1/3}$ ) and was introduced in detail in the first part of this article [7]. When the lamella thickness is plotted as a function of the crystallinity x detected from volumetric [3,6,9] or calorimetric experiments [11,12], a correlation is evident. The different data in literature agree fairly well and can be described with a 3<sup>rd</sup> order polynomial [10].

The dependence of the lamella thickness  $l_c$  on the molar mass [3,9] can be understood as a consequence of the molar mass dependence of the crystallization rate [9,10,13]. As crystallization necessarily requires molecular mobility, the lamella thickness  $l_c$  is also significantly influenced by the relaxation time scale [9,10]. As the motions during crystallization are occurring on a rather small scale, despite the high speed of crystallization, mainly very low shear rates should occur. Thus, the zero shear-rate viscosity  $\eta_0$  should be a better influence factor for the lamella thickness than the molar mass. For linear polymers, this does not matter very much as  $\eta_0$  and  $M_w$  are proportional to each other (e.g. [14-16]). However, the zero shear-rate viscosity of long-chain branched polymers is not only dependent on  $M_w$  but also on the branching topography (number of long-chain branches, their length, position, ...) [16-21].

Piel et al. [18] showed that for HDPE without any comonomer the crystallinity obtained after cooling with a cooling speed of 20 K/min varies between approximately 70% ( $M_w \approx 70$  kg/mol) and 44% ( $M_w \approx 1,000$  kg/mol).

The  $\alpha$ -relaxation is only observed in samples with a morphology type IV according to the morphology scheme developed for ethene-/ $\alpha$ -olefin-copolymers [19].

<sup>†</sup>To whom correspondence should be addressed.  
E-mail: fjadler@jbnu.ac.kr

<sup>\*</sup>This paper is dedicated to Professor Ki Ju Kim for celebrating his retirement from Division of Chemical Engineering of Chonbuk National University

**Table 1. Literature data of activation energies for  $\alpha$ - and  $\beta$ -relaxations, SCB - short chain branched, lin - linear**

| Author                   | $E_a$ ( $\alpha$ ) [kJ/mol] | $E_a$ ( $\beta$ ) [kJ/mol] | Branches | Method  |
|--------------------------|-----------------------------|----------------------------|----------|---|
| Matthews et al. [12]     | 80-120                      | 430-500                    | SCB      | Temperature dependent maximum of $\tan\delta$ (0.1-30 Hz) |
| Nitta and Tanaka [3]     | -                           | 200-250                    | SCB      | $\log a_T$ (unknown frequency spectrum)                   |
|                          | 100-120                     | 90                         | lin      |   |
| Głowinkowski et al. [25] | 75-88                       | 50                         | SCB, lin | NMR   |

$\alpha$ -octene- and ethene/styrene- copolymers [1]. This scheme is also applicable for other ethene/ $\alpha$ -olefin copolymers, although the correlation between the comonomer content and the resulting crystallinity will be different. As an example, the border between morphology type III and IV is around 55% ( $x_v^{1/3}=0.82$ ) crystallinity or 2.5 mol% comonomer in case of a homogeneous comonomer distribution, while for an inhomogeneous comonomer distribution, the border can be somewhat higher due to the partial phase separation of PE chains with different comonomer contents [9,10,22,23]. The effect of side-chain distribution on the crystallization has recently been shown by Wagener's group [24] - the broadening of the melting peak in pure random copolymers is, therefore, mainly caused by chain segments with different lengths between the short-chain branches. The comonomer content and distribution influences the  $\alpha$ -transition indirectly, as it produces short-chain branches (SCB), which influence the crystallinity and morphology.

The activation energy of the  $\alpha$ -relaxation has been measured by several authors (Table 1). Matthews et al. [12] found activation energies of the  $\alpha$ -relaxation for SCB-polyethylenes between 80 and 120 kJ/mol, which were determined by dynamic-mechanical measurements at a constant heating rate on frequencies ranging between 1 and 30 Hz, i.e., heating scans on different samples. Nitta and Tanaka [3] determined the activation energy for linear and SCB-polyethylenes to have values between 100 and 120 kJ/mol, however, without stating how they exactly determined the shift factors. Głowinkowski et al. [25] used nuclear magnetic resonance (NMR) and determined identical activation energies of the  $\alpha$ -relaxation of linear and SCB-polyethylenes to about 80 kJ/mol. The data found in literature indicates that the activation energy should be between 75 and 120 kJ/mol for a typical HDPE.

However, it is still somewhat illusive, when the  $\alpha$ -relaxation is taking place and which structural factors influence it (besides the lamella thickness).

The  $\beta$ -relaxation is located in the amorphous phase as it is found in completely amorphous ethene/ $\alpha$ -olefin copolymers, too (e.g. [26]). From the dependence of the intensity of the relaxation measured in  $\tan\delta$  on the crystallinity, Starck and Löfgren [27] concluded that the origin of the  $\beta$ -relaxation is in the amorphous phase. Dechter et al. [28] drew the same conclusion from their NMR-measurements as the mobility of the chains in the amorphous regime is quite high, while the chains in the crystallites are almost fixed.

In linear HDPE, the  $\beta$ -relaxation is reported to be very weak or not to be observable at all. Matthews et al. [12] concluded that this is due to the high degree of crystallinity. The crystal lamellae hinder the small amorphous phase to undergo the  $\beta$ -relaxation until the  $\alpha$ -transition has occurred. Therefore, the  $\beta$ -transition is not observable, as it overlaps with the  $\alpha$ -transition occurring at the very same temperature.

All articles found agree that the  $\beta$ -relaxation takes place in short

chain branched polyethylenes (LLDPE and LDPE) between  $-60$  and  $+20$  °C. Its intensity is strongly connected to the crystallinity. According to Starck and Löfgren, the intensity of the  $\beta$ -transition is not only dependent on the size of the interfacial phase [29] but also on the type of comonomer [27].

The activation energy of the  $\beta$ -transition was reported several times (Table 1). Matthews et al. [12] found values between 430 and 500 kJ/mol for an LLDPE subjected to different thermal and mechanical treatments but showing a crystallinity of around 40%. Nitta and Tanaka [3] report values between 200 and 250 kJ/mol for quenched LLDPE with crystallinities between 35 and 43%. For quenched HDPE with crystallinities between 70 and 54%, they found activation energies of around 90 kJ/mol in the region of the weak  $\beta$ -transition. Głowinkowski et al. [25] found an activation energy of the  $\beta$ -relaxation of 50 kJ/mol for both an HDPE and an LLDPE.

The strong dependence of the  $\beta$ -relaxation temperature on the comonomer content (and thus on the crystallinity) indicates that it is based on a larger scale movement.

The values reported for the activation energy vary by a factor of 10. The reason may be that this transition is very much dependent on the microstructure of the polymer. It also depends on the method used for the determination of the activation energy.

Although both  $\alpha$ - and  $\beta$ -transition were investigated by several research groups, it is still not completely understood how crystal morphology (lamella thickness, crystal structure, crystallinity, ...) and the relaxations interact. Especially, the broad range of the activation energies found for the  $\beta$ -transition and large temperature span, which is reported, raises the question of what the influencing factors are and is the process the same for all crystallinities. Also, it is not clear from literature whether the activation energy of the  $\alpha$ -relaxation is dependent only on the crystallinity or if other morphological properties come into play.

This article intends to shed some light on these questions to contribute to the clarification of the molecular mechanisms and their link to crystalline structure.

It is also unclear whether the  $\beta$ - or the  $\gamma$ -transition (occurring around  $-115$  °C) can be considered to be the glass transition of PE. This question, however, will be discussed in part III [1] of this article series, as it also requires a thorough discussion of the  $\gamma$ -relaxation.

## EXPERIMENTAL

The  $\alpha$ - and  $\beta$ -relaxation were investigated for a number of commercially available grades of polyolefins. Their thermal characteristics are summarized in Table 2. Experimental details of the sample preparation and measuring techniques used are described in part I of this article series in detail [7] as well as their microstructure. Some rheological data about these samples have been published elsewhere as well [14,15,30-35].

**Table 2. Melting temperatures, densities, and crystallinities for the grades investigated**

| Name     | Quenched samples               |                                     |                         |             |             | Slowly cooled samples          |                                     |                         |             |             |
|----------|--------------------------------|-------------------------------------|-------------------------|-------------|-------------|--------------------------------|-------------------------------------|-------------------------|-------------|-------------|
|          | Melting temperature $T_m$ [°C] | Density $\rho$ [g/cm <sup>3</sup> ] | Crystallinity $x_v$ [%] | $L_p^b$ [Å] | $l_c^b$ [Å] | Melting temperature $T_m$ [°C] | Density $\rho$ [g/cm <sup>3</sup> ] | Crystallinity $x_v$ [%] | $L_p^b$ [Å] | $l_c^b$ [Å] |
| HDPE 1   | 139.6                          | 0.947                               | 70                      | n.d.        | n.d.        | 139.4                          | 0.970                               | 80                      | 270         | 212         |
| HDPE 2   | 135.0                          | 0.940                               | 63                      | 210         | 132         | 135.1                          | 0.949                               | 68                      | 252         | 172         |
| HDPE 3   | 133.2                          | 0.937                               | 61                      | 215         | 145         | 133.6                          | 0.948                               | 68                      | 259         | 181         |
| HDPE 4   | 133.9                          | 0.933                               | 58                      | 255         | 147         |                                |                                     |                         |             |             |
| LLDPE 1  | 124.1                          | 0.919                               | 48                      | 196         | 95          |                                |                                     |                         |             |             |
| LLDPE 2  | 115.3/123.0 <sup>a</sup>       | 0.915                               | 45                      | 172         | 78          |                                |                                     |                         |             |             |
| LDPE 1   | 110.4                          | 0.915                               | 45                      | 134         | 60          | 110.4                          | 0.919                               | 48                      | 152         | 73          |
| LLDPE 3  | 115.8                          | 0.913                               | 44                      | 161         | 70          |                                |                                     |                         |             |             |
| LLDPE 4  | 112.2                          | 0.910                               | 42                      | 155         | 64          |                                |                                     |                         |             |             |
| LLDPE 5  | 106.7                          | 0.904                               | 37                      | 150         | 56          |                                |                                     |                         |             |             |
| LLDPE 6  | 101.4                          | 0.898                               | 33                      | 145         | 48          |                                |                                     |                         |             |             |
| LLDPE 7  | 100.4                          | 0.898                               | 33                      | 138         | 46          | 100.9                          | 0.901                               | 35                      | 143         | 50          |
| LLDPE 8  | 97.8                           | 0.897                               | 32                      | 143         | 46          | 96.9                           | 0.902                               | 36                      | 150         | 60          |
| LLDPE 9  | 94.0                           | 0.896                               | 32                      | 134         | 43          |                                |                                     |                         |             |             |
| LLDPE 10 | 97.1                           | 0.893                               | 30                      | 136         | 41          |                                |                                     |                         |             |             |
| LLDPE 11 | 44.1/63.5 <sup>a</sup>         | 0.871                               | 13                      | 144         | 19          |                                |                                     |                         |             |             |

<sup>a</sup>Two discrete melting peaks were observed; for further analysis the average value of the two values was taken

<sup>b</sup>From [9,10]

The long period  $L_p$  was determined from SAXS-experiments, published in detail elsewhere [9]. The lamella thickness  $l_c$  is calculated from the long period  $L_p$  and the volumetric crystallinity  $x_v$  by

$$l_c = x_v \cdot L_p \quad (1)$$

## RESULTS AND DISCUSSION

### 1. $\alpha$ -Transition

The  $\alpha$ -transition is mainly observed in the HDPE resins showing a crystallinity  $x_v$  of or more than 55%. For LLDPEs no distinct  $\alpha$ -relaxation is found. The differences in the relaxation behavior between the different grades are small compared to the other resins.

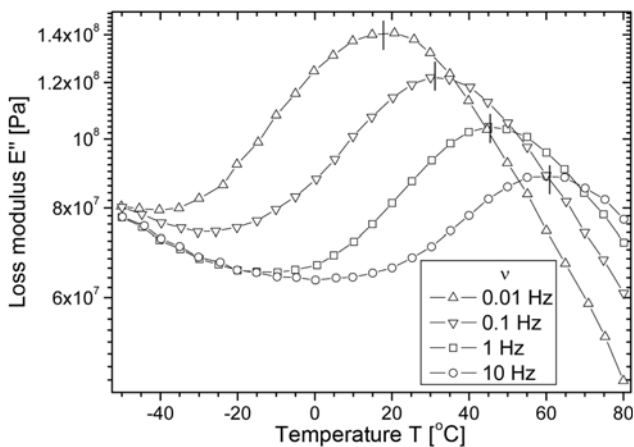


**Fig. 1.**  $\alpha$ -Relaxation of quenched HDPE 2. The vertical line indicates the maximum at each frequency  $\nu$ .

A typical example of an  $\alpha$ -relaxation is given in Fig. 1. This figure shows the loss modulus as a function of temperature at four different frequencies for quenched HDPE 2. A distinct maximum in  $E''$  is observed, which is shifted to higher temperatures with increasing frequency. Besides, the maximum value in  $E''$  decreases with increasing frequency. The different maximum values of the loss modulus  $E''$  at the peak temperature are due to the decrease of the complex modulus in that temperature range [36].

As both the storage and loss modulus decrease in the temperature range at the  $\alpha$ -transition,  $\tan \delta$  does not show a distinct maximum, when plotted at constant frequency as different temperatures.

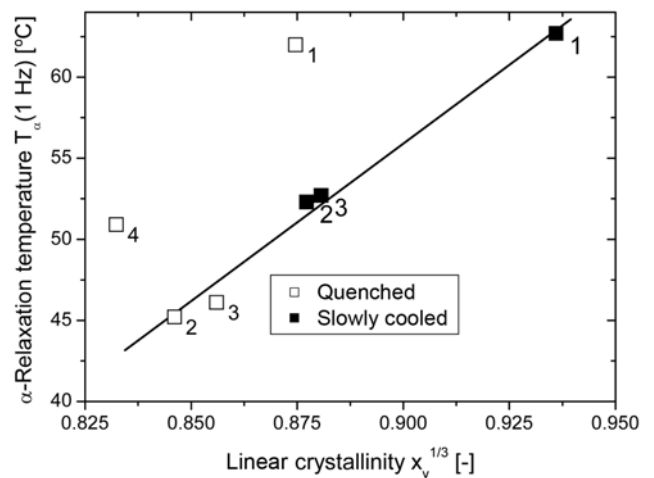


**Fig. 2.**  $\alpha$ -Relaxation temperature of linear HDPE as a function of the linear crystallinity (numbers denote the HDPE sample number).

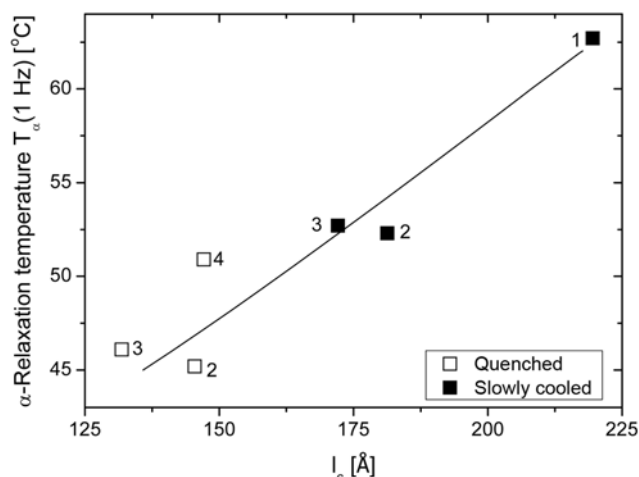


Fig. 3.  $\alpha$ -Relaxation temperature of HDPE as a function of the lamella thickness  $l_c$  (number denotes the HDPE sample number, lamella thickness taken from [10]).

Therefore, the loss modulus was chosen to get an insight into the relaxation mechanisms.

The relaxation temperature was determined as the null of the first derivative of  $E''$  [37] with respect to temperature. Fig. 2 shows that the  $\alpha$ -relaxation temperature at 1 Hz ( $T_\alpha(1 \text{ Hz})$ ) is directly proportional to the linear crystallinity of the sample. Only the quenched samples of HDPE 1 and 4 lie away from the line.

This deviation of quenched HDPE 1 and 4 is due to their different crystallization kinetics, which lead to different lamella structures to be discussed later.

From the findings of Liu et al. [8] and Popli et al. [6] this result is expected, as the  $\alpha$ -relaxation temperature is connected to the crystal lamella thickness and, therefore, to the melting temperature. Thick lamellae (high melting temperature) results in a stronger hindrance of the molecular motion (shear movements along the c-axis being perpendicular to the lamellae) underlying the  $\alpha$ -relaxation. To compensate for the hindrance stemming from the increased lamella stiffness the temperature has to be increased in order to soften the lamellae, thus rendering the  $\alpha$ -relaxation possible.

The best correlation between the  $\alpha$ -relaxation temperature and a structural parameter is found for the lamella thickness  $l_c$ . This confirms Boyd's postulate [4,5] that the  $\alpha$ -relaxation mainly depends on the lamella thickness due to the lamella shear process. The samples follow a linear correlation between those quantities within an error margin of approximately  $\pm 10\%$  in the determination of the lamella thickness  $l_c$ .

From the plot of the frequency of the maximum in  $E''$  in isothermal frequency sweeps (see Fig. 1) as a function of the reciprocal

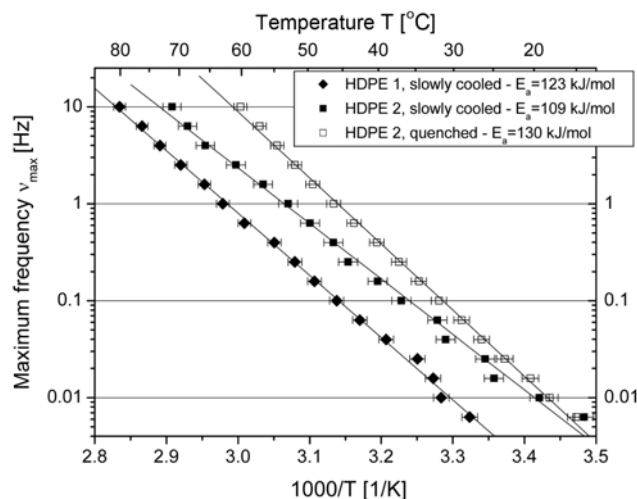


Fig. 4. Arrhenius plot of  $\alpha$ -relaxations of the maximum frequency in  $E''$  of two HDPE with different cooling conditions, the temperature error bars correspond to an uncertainty of  $\pm 1 \text{ K}$ .

absolute temperature (Fig. 4), the activation energies of the  $\alpha$ -relaxation are determined from the maximum of  $E''(T)$  at constant frequency  $\nu$ . They are in the range of 110–120 kJ/mol for the slowly cooled products, while the quenched ones lie a little higher (120–130 kJ/mol). The  $\alpha$ -relaxation of the quenched samples is at lower temperatures but with higher activation energies.

The most probable reason for these slightly higher activation energies is that the lamellae of the quenched samples are more distorted. Thus, their  $\alpha$ -relaxation takes place at a lower temperature, which increases the potential barrier. Unlike in better ordered lamellae of slowly-cooled samples, this barrier can be overcome at that lower temperature because of the more imperfect crystal structure.

The data for the activation energies and the  $\alpha$ -transition temperatures are given in Table 3.

The quenched samples HDPE 3 and 4 represent special cases of the  $\alpha$ -relaxation and are, thus, discussed later (cf. Fig. 10–12).

## 2. $\beta$ -Transition

The  $\beta$ -relaxation was found in all LLDPEs, plastomers and LDPEs.

As an example, Fig. 5 shows the  $\beta$ -relaxation in  $E''$  at 1 Hz of three quenched LLDPE-products. The  $\beta$ -transition temperature was determined as the maximum of the loss modulus as a function of temperature ( $E''(T)$ ) at a fixed frequency (just like the  $\alpha$ -transition). Fig. 5 compares LLDPEs of different crystallinity and different morphologies. LLDPE 1 has the highest crystallinity (48%) with a type III morphology, while LLDPE 9 has a type II morphology and a crystallinity of 32%. The sample LLDPE 11 is almost amorphous

Table 3.  $\alpha$ -Relaxation temperatures and activation energies

| Name   | Quenched samples            |                        |                         | Slowly cooled samples       |                        |                         |
|--------|-----------------------------|------------------------|-------------------------|-----------------------------|------------------------|-------------------------|
|        | $T_\alpha(1\text{Hz})$ [°C] | $E_a(\alpha)$ [kJ/mol] | Crystallinity $x_v$ [%] | $T_\alpha(1\text{Hz})$ [°C] | $E_a(\alpha)$ [kJ/mol] | Crystallinity $x_v$ [%] |
| HDPE 1 | 62                          | 124                    | 67                      | 63                          | 123                    | 82                      |
| HDPE 2 | 45                          | 130                    | 61                      | 52                          | 109                    | 68                      |
| HDPE 3 |                             |                        |                         | 53                          | 121                    | 68                      |

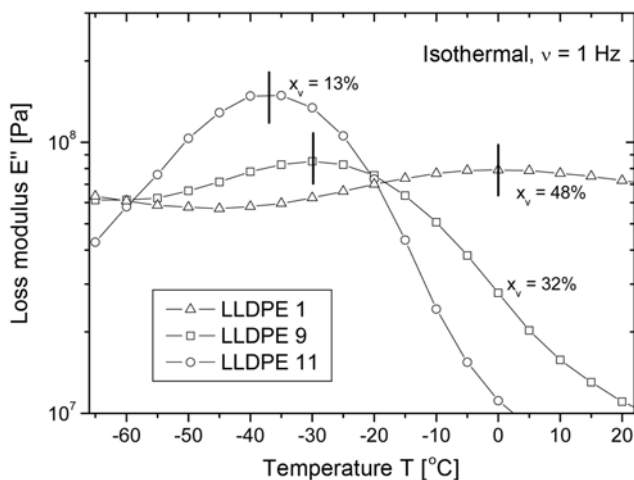


Fig. 5.  $\beta$ -Relaxation of three quenched LLDPEs at 1 Hz. Relaxation temperatures are marked by vertical lines.

( $x_v=13\%$ ) with a type I morphology. The maximum broadens with increasing crystallinity and is shifted to higher temperatures. An increase in crystallinity not only decreases the amount of the amorphous phase, but simultaneously decreases the mobility of the molecules in the amorphous region, as the average distance between chains and thus the local free volume is reduced [10]. As the mobility of polymer molecules in the amorphous state is governed by both the temperature and the free volume, the temperature has to be increased to attain the chain mobility necessary for the  $\beta$ -transition.

The broadening of the transition on temperature scale with increasing crystallinity can be explained by the assumption of a non-uniform distribution of the chain mobility in the amorphous phase between the crystallites, which is caused by the different proximities to the next crystal. In a sample with a rather low crystallinity, these effects do not play a decisive role, while in LLDPE with a crystallinity around 50%, the chains in the amorphous phase close to the crystallites should be much less mobile than the ones farther away from it.

Assuming that the boundary between the crystals and the amorphous region is gradual, it becomes obvious that the amorphous regime between the crystal lamellae is not very large. This can be easily understood from the following example. For PE with a crystallinity between 20 and 60% and a molar mass  $M_w$  around 100 kg/mol (which is typical for commercial LLDPE extrusion grades), a nearly constant interlamellar spacing of approximately 95 Å was found, which is equivalent to 37 monomer stretched units [10]. As the size of the crystallites and their distance from each other are not uniform, the amorphous phase will statistically fluctuate in size. The higher the crystallinity the more rigid the crystallites will be. Therefore, the chain segments in the amorphous phase in proximity to the crystallites will have a reduced mobility, while the ones far away from it are much less restricted in terms of mobility. This leads to a gradient of chain mobility in the amorphous phase as a function of distance from the crystal interface. The size of this gradient is highly dependent on the rigidity of the crystal.

Therefore, it is understandable that the peaks of the  $\beta$ -transitions in Fig. 5 are broadened and decreased in intensity. This also provides a possible explanation for the fact that no  $\beta$ -relaxation was

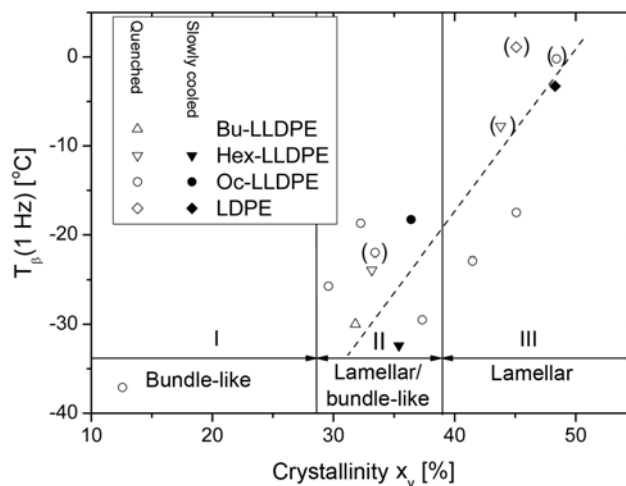


Fig. 6.  $\beta$ -Relaxation temperature ( $T_\beta$  (1 Hz)) as a function of the crystallinity (data points determined in 3.3). Line is least square fit to the data with morphology type II and III. The data points in brackets represent special cases to be discussed in Fig. 10-12.

found for samples with a type IV-morphology; the reduced interlamellar spacing and the rigidity of the crystallites lead to a very much reduced chain mobility in the amorphous phase and, hence, to a distinct weakening of the  $\beta$ -relaxation along with a even more pronounced broadening of the relaxation peak. This will lead to a disappearance of the relaxation in DMTA-measurements. The  $\beta$ -relaxation, however, still exists in these samples—it is just that much smeared out that it cannot be detected anymore. Also, it is partially overlapped by the  $\alpha$ -, the  $\alpha'$ -relaxation and the onset of the melting peak. One has to consider that the content of amorphous material decreases with increasing crystallinity and, thus, also the intensity of the  $\beta$ -transition.

When plotting the  $\beta$ -relaxation temperature  $T_\beta$  (1 Hz) vs. the crystallinity, a linear decrease with decreasing crystallinity is evident for type II and III morphologies (Fig. 6), which is in agreement with literature [1,3,26,27]. The transition temperature seems not to depend on the thermal history of the sample and is also independent of the comonomer type. A plot of  $T_\beta$  (1 Hz) vs. the comonomer content (not shown) shows the same tendency. However, the data deviates from a linear dependence  $T_\beta(x_i)$  by up to 15 K in the  $\beta$ -relaxation temperature. Therefore, other properties also have to play a role.

The morphology classes according to Bensason et al. [1] are indicated in the plot, too. It seems that polyethylenes with a type III morphology feature  $\beta$ -transition (at 1 Hz) temperatures between 0 and  $-25^\circ\text{C}$ . Polyethylenes having with a type II morphology have a transition temperature between  $-18$  and  $-30^\circ\text{C}$ . For polyethylenes with a type I morphology  $T_\beta$  (1 Hz) comes to lie even below that temperature. However, this cannot be discussed in a quantitative way as only one sample lies in that region. Mäder et al. [26] found the  $\beta$ -relaxation temperature of amorphous ethene-/butene copolymers with comonomer contents between 31 and 56 mol% to be around  $-60^\circ\text{C}$ . This small temperature dependence for the amorphous samples and the relatively large one for the crystalline samples indicates that the crystalline structure at least partially determines the  $\beta$ -relaxation temperature. The most likely process for that

is the reduction of chain mobility in the proximity of the crystals, which obviously is irrelevant for amorphous samples.

For the samples with crystallinities between 30 and 50% a linear dependence of  $T_{\beta}$  (1 Hz) on  $x_v$  was fitted, describing all data points with an accuracy of  $\pm 10$  K:

$$T_{\beta}(1 \text{ Hz}) = T_{\beta}^0(1 \text{ Hz}) + S_{\beta} \cdot x_v \text{ for } x_v > 30\% \quad (2)$$

$S_{\beta}$  is called the sensitivity of the  $\beta$ -transition temperature. The fit supplies values of  $T_{\beta}^0 = -70.8$  °C and  $S_{\beta} = 1.4$  K per % crystallinity.

Three resins from the same manufacturer are comparable in all properties except for the comonomer type used (LLDPE 7, 8, and 9) and are within the same morphology class II. The comonomer content of the samples is approximately equal to  $6.5 \pm 1$  mol%. The crystallinity of LLDPE 8 and 9 is the same ( $x_v = 32\%$ ), while LLDPE 7 shows a slightly higher crystallinity of 33%. This is the consequence of the higher effectivity of longer comonomers in suppressing the crystallization.

The Arrhenius plot of these resins is shown in Fig. 7. The activation energy ( $\approx 235$  kJ/mol) is similar for all these polymers within an error margin of 10%. A possible correction for the differences in crystallinity of LLDPE 7 using the scaling law (2) is within the limits of uncertainty. Fig. 7 shows that at a fixed frequency an in-

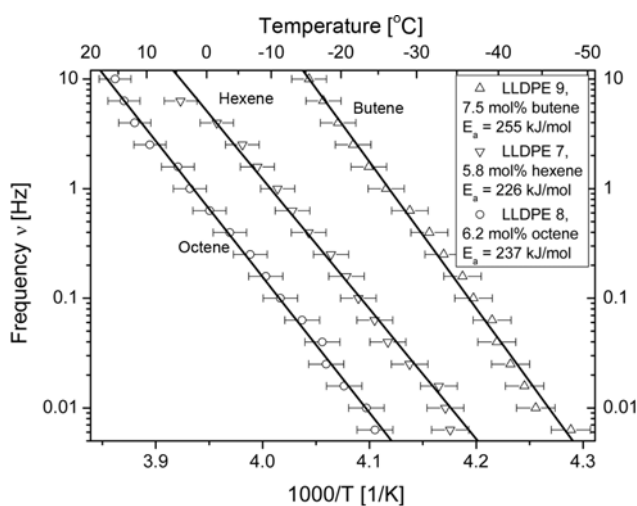


Fig. 7. Arrhenius plot of the  $\beta$ -relaxation of three quenched LLDPE-plastomers with different comonomer but similar crystallinity (for further details see text).

crease in comonomer length results in an increase in  $T_{\beta}$  (1 Hz). The data suggests that each additional  $\text{CH}_2$ -group in the comonomer increases  $T_{\beta}$  by about 7 K. Starck and Löfgren [27] describe the same effect for the longer comonomers octene, tetradecene (C14), and octadecene (C18), but found that a further increase of the comonomer length leads to an increase of  $T_{\beta}$ , which is in agreement with the findings of Piel et al. [38], who found that longer comonomers tend to cause a side chain crystallization.

As the crystallinities of LLDPE 8 and 9 are the same, while the comonomer contents are 6.2 mol% octene and 7.5 mol% butene, respectively, it is concluded that longer comonomers are more effective in decreasing the  $\beta$ -transition temperature. This is easily imaginable by considering the sterical obstruction of comonomers with different chain lengths during crystallization.

Although most samples studied have similar activation energies of the  $\beta$ -relaxation between 200 and 250 kJ/mol, some samples exhibit a much higher activation energy. Fig. 8 shows the Arrhenius plots of those samples together with some typical examples.

The activation energy of the  $\beta$ -transition of all samples determined from the Arrhenius plots is summarized in Table 4. At a first glance, the broad range of activation energies in literature (Table 1) is confirmed and also certain commonalities can be derived. For some of the samples a very unusual thermal behavior was found, which will be discussed later.

When looking at the activation energies as a function of crystal-

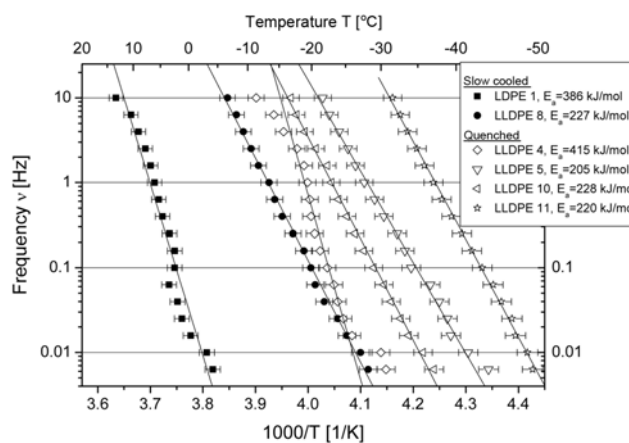
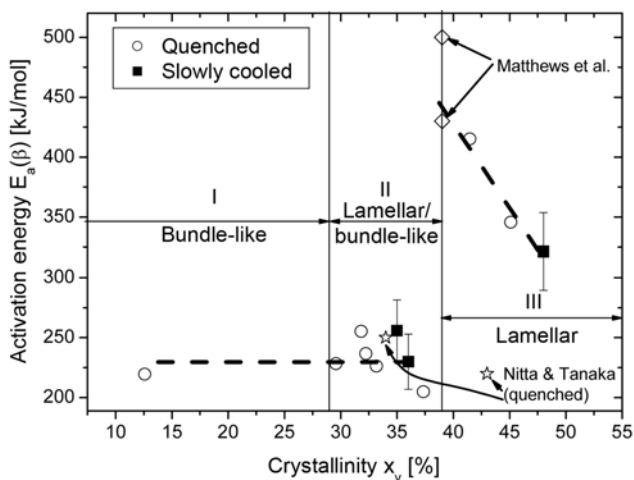


Fig. 8. Arrhenius-plot of the  $\beta$ -relaxations of an LDPE and some LLDPE products.

Table 4.  $\beta$ -Relaxation temperatures and activation energies

|          | Morphology class | Quenched samples        |                            |                         | Slowly cooled samples   |                            |                         |
|----------|------------------|-------------------------|----------------------------|-------------------------|-------------------------|----------------------------|-------------------------|
|          |                  | $T_{\beta}$ (1 Hz) [°C] | $E_a$ ( $\beta$ ) [kJ/mol] | Crystallinity $x_v$ [%] | $T_{\beta}$ (1 Hz) [°C] | $E_a$ ( $\beta$ ) [kJ/mol] | Crystallinity $x_v$ [%] |
| LLDPE 2  | III              | -18                     | 346                        | 45                      |                         |                            |                         |
| LDPE 1   | III              |                         |                            |                         | 1                       | 322                        | 48                      |
| LLDPE 4  | III              | -23                     | 415                        | 42                      |                         |                            |                         |
| LLDPE 5  | II               | -30                     | 205                        | 37                      |                         |                            |                         |
| LLDPE 7  | II               | -24                     | 226                        | 33                      | -32                     | 256                        | 35                      |
| LLDPE 8  | II               | -19                     | 237                        | 32                      | -18                     | 230                        | 36                      |
| LLDPE 9  | II               | -30                     | 255                        | 32                      |                         |                            |                         |
| LLDPE 10 | II               | -26                     | 228                        | 30                      |                         |                            |                         |
| LLDPE 11 | I                | -37                     | 220                        | 13                      |                         |                            |                         |



**Fig. 9.** Activation energies of the  $\beta$ -relaxation as a function of the crystallinity (only including  $\beta$ -relaxations without a bend in the Arrhenius plot), a 10% error is shown for the slowly cooled samples.

linity and of morphology class, they are grouped as follows: the activation energy of the  $\beta$ -relaxation of a polymer with a type III morphology is 300–450 kJ/mol, while the bundle crystallite dominated morphologies I and II have activation energies between 200 and 260 kJ/mol (Fig. 9). These results suggest a slightly other value for the border between type II and III morphology. It was changed from  $x_v=43\%$  as suggested by [1] to 39% [39] based on the activation energies found here and also by Matthews et al. [12] and Nitta and Tanaka [3]. However, the data point with a crystallinity of 42% of Nitta and Tanaka [3] does not follow the tendency of the other data points, as its activation energy is much lower than the values of the comparable samples LLDPE 2 and 4.

It is interesting to note that the activation energy is found to increase for samples with a type III morphology with decreasing crystallinity. At the border between type II and III morphology ( $x_v \approx 39\%$ ), the activation energy of the  $\beta$ -transition is expected to reach a maximum of about 450 kJ/mol. This value is reached by Matthews et al. [12].

This can be explained by distorted crystalline lamellae which are no longer sufficiently strong to prevent the  $\beta$ -relaxation from happening at low temperatures, but they are strong enough to double the potential barrier compared to samples with a type II morphology. Hence, a mixed type II and III morphology causes an extremely high activation energy of the  $\beta$ -relaxation. It is interesting to note that the maximum value of  $E''$  shows a similar behavior to the activation energy, although increasing with decreasing crystallinity, which is due increasing fraction of chains being able to do the  $\beta$ -relaxation, i.e., amorphous chains.

The samples with type II and I morphologies have activation energies around 230 kJ/mol independent of their crystallinity. This suggests that the number and size of bundle crystallites and lamellae does not influence the potential barrier. The size of the lamellae/bundles around  $x_v \approx 39\%$  is approximately 60 Å. As stated before, the interlamellar spacing in this regime is around 95 Å remaining constant down to crystallinities around 20% [10].

In HDPE, this transition was observed to be very weak accord-

ing to literature. In our measurements, we were not able to observe it as a separate relaxation for any PE. Thus it is not possible to discuss this issue quantitatively.

**3. Overlapping  $\alpha$ - and  $\beta$ -transitions**

The activation energies of the relaxations were determined by using the temperatures of the peak maximum of the loss modulus at various fixed frequencies. As long as only one relaxation process is dominant, the activation energy can be determined easily with this method. If a broad or even bimodal peak is present in  $E''$  two or more molecular processes overlap. As relaxations of different molecular origin normally have different frequency dependencies, the shape of the peak changes with frequency. If the relaxation process changes within the frequency range applied in the DMTA-tests, the Arrhenius plot will exhibit different activation energies at different frequencies. The result is an Arrhenius plot having two linear branches of different slope.

Fig. 10 shows the  $\alpha$ -relaxation of the quenched HDPE 3. All frequencies between 0.016 and 0.6 Hz show a broad peak with high

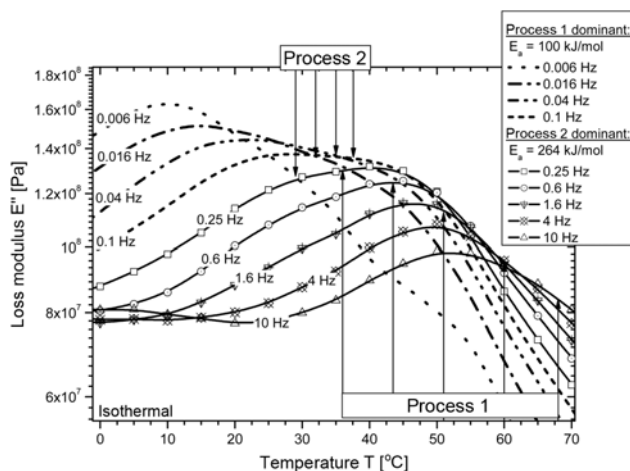


**Fig. 10.** Temperature dependence of loss modulus of HDPE 3 (quenched) at various frequencies showing two overlapping relaxation processes. The arrows marking the non-dominant process (details of the determination see text).

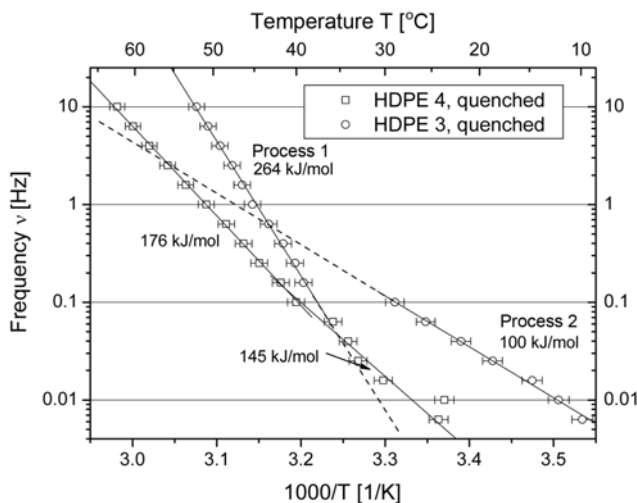


**Fig. 11.** Arrhenius plot of the  $\alpha$ -relaxation of HDPE 3 and HDPE 4.

(e.g., 0.006 Hz) or low temperature shoulders (0.25 Hz). The change in peak shape is a strong indication of the presence of two processes. In the Arrhenius plot, where only the maximum temperature is plotted (Fig. 11), these two processes are clearly distinguishable because two straight lines of different slope (activation energy) are evident.

For quenched HDPE 3 very pronounced differences in the activation energies are visible in Fig. 11. Process 1 takes place at higher temperatures with an activation energy of 265 kJ/mol, while the second process is found at a lower temperature with a significantly lower activation energy of 100 kJ/mol. Additionally, no peaks are found between 30 °C and 40 °C. For quenched HDPE 4 the difference in the activation energies is rather low so that it would be possible to consider this effect as a measurement error. The data of quenched HDPE 3, however, make this unlikely.

For quenched HDPE 3, the temperature of the peak maxima for each process was calculated from the activation energies (Fig. 10), the relaxation for all the frequencies where the respective process is not dominant. Its relaxation temperature was marked in Fig. 10 as an arrow. The relaxation temperatures of process 1 are marked with upward pointing arrows; downward pointing arrows were used for process 2. Especially, the maxima of process 2 are evident at low frequencies as a broad maximum or shoulder, even though process 1 is dominant. HDPE 4 shows the same effect but with smaller differences. Only at low frequencies is a broadened relaxation peak observable.

It should be mentioned that slowly cooled HDPE 3 showed an unusual scattering behavior in WAXS and SAXS, which was attributed to intermolecular phase separation as a consequence of two distinctly different species of chains with virtually no and significant amounts of comonomer [9,10]. However, the question remains, how this phase separation affects the quenched sample discussed here, where no distinct phase separation is found.

A similar observation was made for some of the  $\beta$ -relaxation as well. Four quenched products (LDPE 1, LLDPE 1, 3, 6) show these two ranges of significantly different temperature dependencies.

The temperature dependence of the  $\beta$ -relaxations of these four products shows an Arrhenius plot (Fig. 12) similar to the  $\alpha$ -relaxation of quenched HDPE 3.

The change in the temperature dependence of the  $\alpha$ - and  $\beta$ -relaxations occurs at frequencies between 0.6 and 0.1 Hz for the six samples showing this effect. Thus the Arrhenius plots (Fig. 11/Fig. 12) showing the two regimes of different temperature dependence are

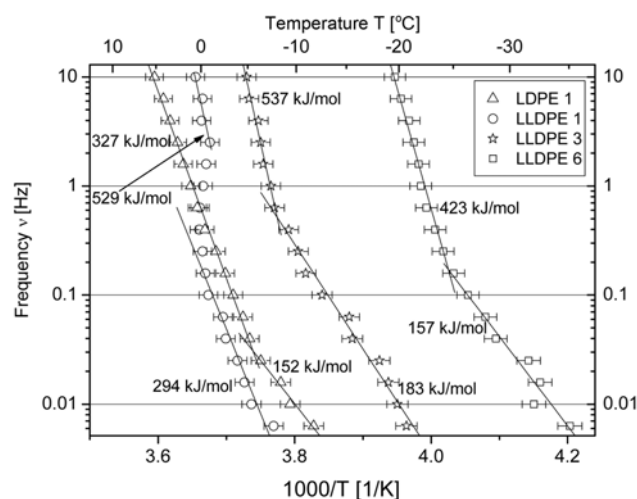


Fig. 12. Arrhenius plot of the  $\beta$ -relaxations of quenched products showing two regions of different activation energies.

documented by at least four measuring points in each region. We, therefore, believe that the effect is real. One reason why this effect has not been described before is that no recent article reported measurements at frequencies below 0.1 Hz.

The activation energies of the two branch transitions and the cross-over frequencies separation of the two branches are listed in Table 5. The open question is now what the nature of the two overlapping relaxation processes is.

Five samples in the crystallinity range of  $60\% > x_c > 44\%$  show two overlapping processes. These samples have crystallinities, which classifies them as morphology type III samples or type IV samples, which are close to a type III morphology [1]. Matthews et al. [12] postulate that the  $\beta$ -relaxation cannot occur in HDPE due to geometrical constraints in the very small amorphous regions between the lamellae. If the  $\alpha$ -relaxation has occurred, the constraints are removed and the  $\beta$ -relaxation can take place now.

Therefore, the assumption is evident that the two processes observed are in fact the  $\alpha$ - and the  $\beta$ -relaxation. The high temperature process with the higher activation energy is attributed to the  $\beta$ -relaxation despite the higher relaxation temperatures; the process with the lower activation energy is the  $\alpha$ -relaxation. This seems contradictory at a first glance; however, it becomes comprehensible, when, additionally, assuming  $T_\alpha$  to be slightly above  $T_\beta$ , the  $\alpha$ -relaxation

Table 5. Activation energies for overlapping  $\alpha$ - and  $\beta$ -relaxations

| Name    | $X_c$ [%] | Activation energy $E_a$ ( $\alpha$ ) - process 1 | Activation energy $E_a$ ( $\beta$ ) - process 2 | Highest frequency of dominating $\alpha$ -relaxation [Hz] |
|---------|-----------|--|---|---|
| HDPE 3  | 61        | 145  | 176   | 0.1   |
| HDPE 4  | 58        | 100  | 265   | 0.1   |
| LLDPE 1 | 48        | 294  | (529) <sup>a</sup>                              | n.d.  |
| LDPE 1  | 45        | 152  | 327   | 0.6   |
| LLDPE 3 | 44        | 183  | 537   | 0.4   |
| LLDPE 6 | 33        | 157 <sup>b</sup>                                 | 423 <sup>b</sup>                                | 0.16 <sup>b</sup>   |

<sup>a</sup>Strange shape of Arrhenius plot, activation energy questionable

<sup>b</sup>Exact origin of process unknown

has to occur below the  $\beta$ -relaxation temperature at low frequencies due to its lower activation energy.

The values of the activation energy  $E_a$  of the overlapping  $\alpha$ -relaxation are higher than found for the samples with the "normal"  $\alpha$ -relaxations and lower in the relaxation temperature (except for quenched HDPE 3). As those samples feature a lower crystallinity and thus a more distorted crystal structure, the argumentation of the influence of quenching in comparison to slowly-cooling can be applied to this finding as well. The activation energies of the overlapping  $\beta$ -relaxations are in the range of those of the samples with normal  $\beta$ -relaxations (see also the dashed lines in Fig. 11).

If the amorphous phase is still frozen, the hindrance of the lamellar  $\alpha$ -relaxation is higher and thus the  $\alpha$ -transition will take place with a higher intensity compared to the  $\alpha$ -relaxation in lamellae surrounded by a rubbery amorphous phase. Therefore, the  $\alpha$ -relaxation found at temperatures below the  $\beta$ -transition will have a higher intensity than those at temperatures above the  $\beta$ -transition, which was found, e.g., for quenched HDPE 3 (Fig. 10). The  $\beta$ -transition, however, is not distinctly influenced by the  $\alpha$ -transition. Thus the  $\alpha$ -transition at temperatures below the  $\beta$ -transitions will show a double peak (in the plot  $E''(T)$ ), while in the opposite case only a small shoulder is found.

In the case of  $T_\beta < T_\alpha$ , part of the deformation can be compensated by the rubbery amorphous phase, thus leading to a diminishing intensity of the  $\alpha$ -relaxation at higher frequencies.

The activation energies of the overlapping relaxations are increased, which is probably due a mutual hindrance of the  $\alpha$ - and the  $\beta$ -relaxation. If the  $\beta$ -relaxation is shifted towards higher temperatures, the potential barrier is increased and thus the activation energy.

This can be observed when looking at Fig. 9, which shows the increase of the activation energy of the  $\beta$ -relaxation as a function of the crystallinity. The  $\beta$ -relaxation is also increased. As a higher crystallinity causes a more ordered crystal structure, the potential barrier increases. As the resins with a type III-morphology feature very narrow amorphous interlamellar areas, the  $\beta$ -relaxation is very much hindered, thus leading to higher transition temperatures.

The potential barrier of the  $\alpha$ -relaxation on the other hand is lowered by the decreasing lamella thickness in a type III morphology. Therefore, the  $\alpha$ -transition is shifted to lower temperatures. As the  $\alpha$ -process requires at least partially rubbery amorphous regions, the transition cannot be shifted much below the  $\beta$ -transition. Thus the  $\alpha$ - and the  $\beta$ -transitions are occurring almost at the same temperatures. Because of the hindrance of the high temperature of the  $\beta$ -relaxation, the activation energy of the  $\alpha$ -relaxation is increased for type III but not for type IV materials.

In case of LLDPE 6, the Arrhenius plot has two regimes which have significantly different activation energies. However, no clear sign of bimodality is found when looking at  $E''(T)$  at fixed frequency  $\nu$ . Also, the temperature of the low frequency regime is much too low to be an  $\alpha$ -transition. According to different experiments with copolymerizations the incorporation of comonomer changes the molar mass and, thus, it is unlikely that a sizable comonomer gradient is present in the material without broadening its molar mass distribution  $M_w/M_n$ , but cannot be completely excluded [19,38,40,41]. This suggests that the two relaxations taking place are indeed two  $\beta$ -relaxations. The relaxation dominant at high frequencies is showing a type III  $\beta$ -relaxation, while the one at low temperatures looks

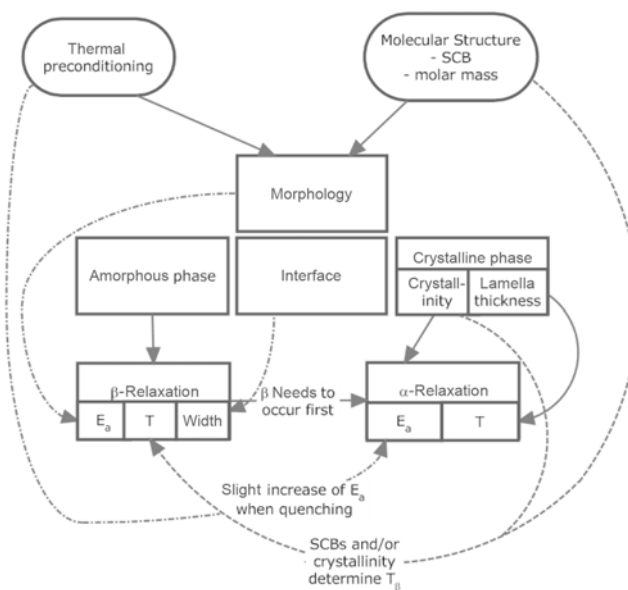


Fig. 13. Overview of the links between molecular structure and different relaxations described in literature.

like a type II  $\beta$ -transition. The conclusion of this finding is very interesting. A sample with a crystal morphology which behaves like type III at high frequencies but like type II at low frequencies must have a morphology, which is at the border between those two crystal morphologies. This means that the border between them is a clear dividing line.

## CONCLUSIONS AND SUMMARY

An overview of the structure property relationships in literature and established in this article is given graphically in Fig. 13.

The  $\alpha$ -relaxation was found in all samples with a crystallinity of above of 55%, which classifies their morphology as type IV (highly ordered lamellar [1]). In some quenched resins with a type III morphology this transition appears also but it is accompanied with the  $\beta$ -transition, at least partially overlapping each other. As the  $\alpha$ -relaxation temperature is decreasing with decreasing crystallinity the origin was confirmed to be the crystal lamellae.

The  $\beta$ -relaxation, on the other hand, originates in the amorphous phase. This is evident because the  $\beta$ -relaxation disappears with increasing crystallinity and so does its activation energy.

Several quenched samples with a crystallinity between 63 and 40% were found to have a bend in the Arrhenius plot of their  $\alpha$ - or  $\beta$ -relaxation. This bend was attributed to overlapping  $\alpha$ - and  $\beta$ -relaxations, whose relaxation temperatures are unchanged compared to a non-overlapped  $\alpha$ - or  $\beta$ -relaxation, but their activation energies are increased due to a mutual hindrance of those two processes.

## ACKNOWLEDGEMENTS

The authors would like to thank Prof. Dr. H. Münstedt, Dr. J. Kaschta (Universität Erlangen-Nürnberg, Germany), Prof. Dr. G. Hartwig (Kernforschungszentrum Karlsruhe, Germany), and Dr. Michaël Mainil (Unité de Physique et de Chimie des Hauts Poly-

mères, Université catholique de Louvain, Belgium) for discussions. This work was supported by the “Human Resource Development (project name: Advanced track for Si-based solar cell materials and devices, project number: 201040100660)” of the Korea Institute of Energy Technology Evaluation and Planning (KETEP) grant funded by the Korea government Ministry of Knowledge Economy.

## REFERENCES

1. S. Bensason, S. Nazarenko, S. Chum, A. Hiltner and E. Baer, *Polymer*, **38**, 3513 (1997).
2. G. Hartwig, *Polymer Properties at Room and Cryogenic Temperatures*, New York: Plenum Press (1994).
3. K. H. Nitta and A. Tanaka, *Polymer*, **42**, 1219 (2001).
4. R. H. Boyd, *Polymer*, **26**, 1123 (1985).
5. R. H. Boyd, *Polymer*, **26**, 323 (1985).
6. R. Popli, M. Glotin, L. Mandelkern and R. S. Benson, *J. Polym. Sci. Part B: Polym. Phys.*, **22**(3), 407 (1983).
7. F. J. Stadler, J. Kaschta and H. Münstedt, *Polymer*, **46**, 10311, DOI: 10.1016/j.polymer.2005.07.099 (2005).
8. J. Liu, F. Zhang, F. Xie, B. Du, Q. Fu and T. He, *Polymer*, **42**, 5449 (2001).
9. F. J. Stadler, T. Takahashi and K. Yonetake, *e-Polymers*, **40**, (2009).
10. F. J. Stadler, T. Takahashi and K. Yonetake, *e-Polymers*, **41**, (2009).
11. R. O. Sirotkin and N. W. Brooks, *Polymer*, **42**, 9801 (2001).
12. R. G. Matthews, A. P. Unwin, I. M. Ward and G. Capaccio, *Journal of Macromolecular Science-Physics*, **B38**, 1-2, 123-143 (1999).
13. L. Mandelkern, *The crystalline state*, 2nd Ed., Chap. 4. Washington DC, ACS (1993).
14. F. J. Stadler and H. Münstedt, *J. Rheology*, **52**, 697, DOI: 10.1122/1.2892039 (2008).
15. F. J. Stadler, C. Piel, J. Kaschta, S. Rulhoff, W. Kaminsky and H. Münstedt, *Rheologica Acta*, **45**, 755, DOI: 10.1007/s00397-005-0042-6 (2006).
16. F. J. Stadler, C. Piel, W. Kaminsky and H. Münstedt, *Macromolecular Symposia*, **236**, 209, DOI: 10.1002/masy.200650426 (2006).
17. C. Gabriel and H. Münstedt, *Rheologica Acta*, **41**, 232-244 (2002).
18. C. Piel, F. J. Stadler, J. Kaschta, S. Rulhoff, H. Münstedt and W. Kaminsky, *Macromol. Chem. Phys.*, **207**, 26, DOI: 10.1002/macp.200500321 (2006).
19. F. J. Stadler, C. Piel, K. Klimke, J. Kaschta, M. Parkinson, M. Wilhelm, W. Kaminsky and H. Münstedt, *Macromolecules*, **39**, 1474, DOI: 10.1021/ma0514018 (2006).
20. W. W. Graessley and J. Roovers, *Macromolecules*, **12**, 959 (1979).
21. J. Roovers and W. W. Graessley, *Macromolecules*, **14**, 766 (1981).
22. R. Godehardt, S. Rudolph, W. Lebek, S. Goerlitz, R. Adhikari, E. Allert, J. Giesemann and G. H. Michler, *J. Macromol. Sci. Phys.*, **B38**, 5-6, 817-835 (1999).
23. R. Adhikari, R. Godehardt, W. Lebek, S. Frangov, G. H. Michler, H. Radusch and F. J. B. Calleja, *Polym. Adv. Technol.*, **16**, 2-3, 156-166 (2005).
24. G. Rojas, E. B. Berda and K. B. Wagener, *Polymer*, **49**, 13-14, 2985-2995, DOI 10.1016/j.polymer.2008.03.029 (2008).
25. S. Głowinkowski, M. Makrocka-Rydzik, S. Wanke and S. Jurga, *European Polym. J.*, **38**, 961 (2002).
26. D. Mäder, J. Heinemann, P. Walter and R. Mülhaupt, *Macromolecules*, **33**, 1254 (2000).
27. P. Starck and B. Löfgren, *European Polym. J.*, **38**, 97 (2002).
28. J. J. Dechter, D. E. Axelson, A. Dekmezian, M. Glotin and L. Mandelkern, *J. Polym. Sci. Part B: Polym. Phys.*, **20**, 641 (1982).
29. The interfacial regime is believed to be a rather thin layer on the border between the crystal lamellae and the amorphous regime.
30. J. A. Resch, F. J. Stadler, J. Kaschta and H. Münstedt, *Macromolecules*, **42**, 5676, DOI: 10.1021/ma9008719 (2009).
31. U. Kefner, H. Münstedt, J. Kaschta, F. J. Stadler, C. S. Le Duff and X. Drooghaag, *Macromolecules*, In press, DOI: 10.1021/ma100705f (2010).
32. X. Chen, F. J. Stadler, H. Münstedt and R. G. Larson, *Journal of Rheology*, **54**, 393, DOI: 10.1122/1.3305721 (2010).
33. U. Kefner, H. Münstedt, J. Kaschta, F. J. Stadler, C. S. Le Duff and X. Drooghaag, *Macromolecules*, **41**(17), 7341, DOI: 10.1021/ma100705f (2010).
34. F. J. Stadler, A. Nishioka, J. Stange, K. Koyama and H. Münstedt, *Rheologica Acta*, **46**, 1003, DOI: 10.1007/s00397-007-0190-y (2007).
35. F. J. Stadler, C. Gabriel and H. Münstedt, *Macromol. Chem. Phys.*, **208**, 2449, DOI: 10.1002/macp.200700267 (2007).
36. In other words, the material behaves thermorheologically complex, as several processes with different activation energies overlap each other. Thus, no master curve can be constructed, but instead a discussion about the relaxation time dependent activation energy would have to be conducted [30,33]. However, this complicated method does not have to be conducted, as  $E''$  is a clearly separable peak, whose activation energy can, therefore, be determined with relative ease from the peak temperature.
37. Determined as the difference quotient.
38. C. Piel, P. Starck, J. V. Seppälä and W. Kaminsky, *J. Polym. Sci. Part A: Polym. Chem.*, **44**, 1600 (2006).
39. This value was adopted, as it is approximately the mean of the crystallinity of the neighboring samples.
40. C. Piel, *Polymerizations of Ethene and Ethene-co-alpha-Olefin: Investigations on Short- and Long-Chain Branching and Structure Property Relationships*. Department of Technical and Macromolecular Chemistry, Vol. Ph. D. Hamburg: University of Hamburg (2005).
41. C. Piel, K. Scharlach and W. Kaminsky, *Macromolecular Symposia*, **226**, 25 (2005).